No Change in the Recent Lunar Impact Flux Required Based on Modeling of Impact Glass Spherule Age Distributions

Ya-Huei Huang[1] [ID], David A. Minton[1], Nicolle E. B. Zellner[2] [ID], Masatoshi Hirabayashi[3] [ID], James E. Richardson[4], and Caleb I. Fassett[5] [ID]

[1]Department of Earth, Atmospheric, and Planetary Science, Purdue University, West Lafayette, IN, USA, [2]Department of Physics, Albion College, Albion, MI, USA, [3]Department of Aerospace Engineering, Auburn University, Auburn, AL, USA, [4]Planetary Science Institute, Tucson, AZ, USA, [5]NASA Marshall Space Flight Center, Huntsville, AL, USA

Abstract The distributions of $^{40}Ar/^{39}Ar$-derived ages of impact glass spherules in lunar regolith samples show an excess at <500 Ma relative to older ages. It has not been well understood whether this excess of young ages reflects an increase in the recent lunar impact flux or is due to a bias in the samples. We developed a model to simulate the production, transport, destruction, and sampling of lunar glass spherules. A modeled bias is seen when either (1) the simulated sampling depth is 10 cm, consistent with the typical depth from which Apollo soil samples were taken, or (2) when glass occurrence in the ejecta is limited to >10 crater radii from the crater, consistent with terrestrial microtektite observations. We suggest that the observed excess of young ages for lunar impact glasses is likely due to limitations of the regolith sampling strategy of the Apollo program, rather than reflecting a change in the lunar impact rate.

Plain Language Summary Lunar regolith samples collected by the Apollo astronauts contain impact glass spherules that record the age of formation in the Ar-Ar isotope dating system. There are as many spherules with measured ages within the last 500 million years as there is in the previous 4 billion years of lunar history, and it has remained a mystery as to whether this is because the impact rate was higher in the recent past, or if there was some process that was biasing these samples toward a young age. We have developed a three-dimensional computer model that simulates the production, transport, destruction, and sampling of impact-generated glass spherules on the Moon. Using reasonable assumptions that are backed up from data on Earth craters, we are able to reproduce the observed excess of young spherule ages seen in the Apollo samples assuming that impact rate has not changed over the last three billion years. We find that the young age bias is only seen because the Apollo samples were collected in the upper few centimeters of the lunar surface. Future glasses collected from the upper few meters of the surface should have ages that better reflect the true rate of impacts over time.

1. Introduction

Most lunar crater chronologies assume that the impact flux in the inner solar system has been constant for the last ~3 Ga (Neukum, 1983; Neukum et al., 2001; Robbins, 2014). Some researchers have suggested that the impact rate over this time period instead increased sometime in the last ~1 Ga (Culler et al., 2000; Fassett & Thomson, 2014; Grieve, 1984; Mazrouei et al., 2015; McEwen et al., 1997; Shoemaker et al., 1990; Vokrouhlický et al., 2017) or possibly declined (Hartmann et al., 2007; Quantin et al., 2007). Impact melts provide one of the most important records for constraining the lunar impact flux. Impact glass spherules, a kind of impact melt product, are up to 1-mm diameter in size and produced by hypervelocity impacts (Delano et al., 1982; Melosh & Vickery, 1991; Reid et al., 1977). The ubiquity of spherules and their age distribution suggests that they are produced in relatively small impacts (e.g., Delano, 1991; Horz & Cintala, 1997; Korotev et al., 2010; Norman et al., 2012; Symes et al., 1998; Zeigler et al., 2006) and therefore are potentially a powerful record of the impact history since the end of the basin-forming epoch at 3.9 Ga (e.g., Tera et al., 1974).

The analysis of lunar regolith soil samples collected from the Apollo 12, 14, 16, and 17 landing sites shows an excess of impact glass spherules with derived $^{40}Ar/^{39}Ar$ ages of <400–500 Ma (Culler et al., 2000; Hui et al., 2009; Levine et al., 2005; Zellner & Delano, 2015; see Figure 1). A straightforward explanation for the excess of impact glass spherules in this period is an increase in the impact flux by a factor of 2–3 during the late
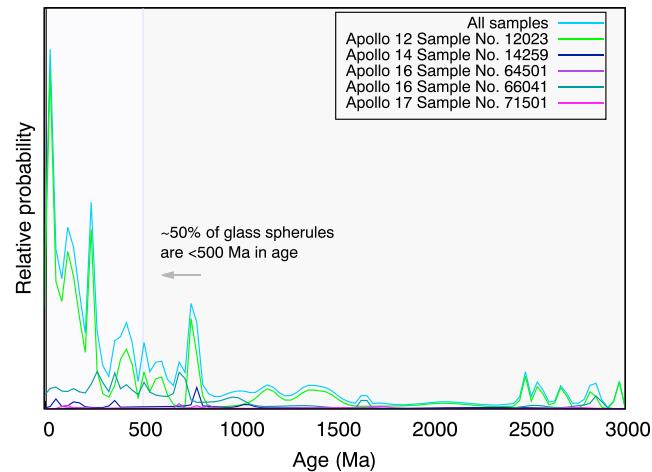
Figure 1. The relative probability plot of five reported lunar regolith samples. The relative impact flux is calculated from the fraction of impact glass spherules and shards normalized by the overall number of impact glass spherules and shards from all five Apollo regolith samples. The data are directly taken from two studies: Zellner and Delano (2015) and Levine et al. (2005). The spherule data of Culler et al. (2000) and Hui et al. (2009) are not included.

Copernican. Because the impact flux is a potentially important factor for biotic evolution on Earth (Alvarez et al., 1980), understanding its history is an important issue. However, it is not known how much the observed age distribution of lunar glass spherules is affected by biases (Hartmann et al., 2007; Hörz, 2000).

A young age bias in the ^{40}Ar/^{39}Ar age distribution of impact glass spherules could arise as a result of several processes. Once formed, spherules in the lunar regolith can be destroyed by subsequent impacts over time, resulting in a preservation bias (Zellner & Delano, 2015). In addition, lunar diurnal temperature cycling may cause argon diffusion of glass spherules exposed on the surface, leading to a lower abundance of argon that is measured as a younger age in a sample (Zellner & Delano, 2015). After accounting for an argon diffusion bias for spherules from several Apollo 14, 16, and 17 regolith samples, Zellner and Delano (2015) show a uniform age distribution over the last one billion years. Even after correcting for a bias arising from diffusive loss of argon, the glass spherules from Apollo 12 12023 regolith still show a prominent spike in the late Copernican (see Figure 1). The geochemical composition data of the Apollo 12 12023 regolith were not available for argon diffusion bias correction, and therefore, further analysis is needed to understand the source of this late Copernican excess of glass ages. This motivates us to seek other possible sources of young age bias that are inherently present in lunar regolith samples.

To date, there is no comprehensive, three-dimensional model that tracks the fate of spherules from the time of their production on the lunar surface through their sampling by the Apollo astronauts. Here we develop a model to understand the expected age distribution of impact glass spherules in the lunar regolith. The model is based on the three-dimensional regolith transport component of the Cratered Terrain Evolution Model (CTEM; Huang et al., 2017; Minton et al., 2015; Richardson, 2009).

In this study, we build off of previous work reported in Huang et al. (2017) in which we implemented a regolith material transport model into CTEM. In our previous study, we only considered a two composition material transport component (basalt and anorthosite). Here we extend the capabilities of the code to track an arbitrary number of distinct regolith components, such as populations of spherules produced at different times. In Huang et al. (2017) we considered how preexisting materials were redistributed by impact craters, but for this work we model the production of spherules by the impacts themselves. Using the new capabilities of the code, we generate the expected age distribution of glass spherules for a model impact flux. We then compare our calculated age distributions of glass spherules with the observed age distribution collected from lunar regolith samples. In our model, we set the impact rate to be constant over the last 3 Ga to show that the excess of spherules with ages of <500 Ma can be due to a sampling bias (see Figure 1). We cannot rule out a possibility of that the lunar impact flux increased; however, we will show the spherule age distribution does not require any temporal change.

2. Materials and Methods

We divide our problem into four model components, which simulate the processes involved in spherule production, transport, destruction, and sampling. In this work *production* refers to the component of the code that models both the total abundance of spherules that are generated in any given impact, and how those spherules are distributed in the ejecta of their source crater. *Transport* refers to the component of the code that models how subsequent impacts redistribute spherules, which makes use of methods developed in Huang et al. (2017). *Destruction* refers to the component of the code that models how impacts destroy old spherules, and *sampling* refers to the way we process the output of our simulations to obtain a representative age distribution of spherules such that we mimic the sampling of lunar regolith by the Apollo astronauts. In this section we give an overview of how each of these model components was implemented and constrained by observations. The supporting information contains more detailed technical descriptions of each of the model components.

2.1. Constraining Lunar Impact Glass Spherule Production

Lunar impact glass spherules form as molten droplets entrained within impact-excavated ejecta during hypervelocity impact cratering events (Delano, 1991; Melosh & Vickery, 1991). In order to model the production of impact glasses within individual lunar impact events in CTEM, we require constraints on both the abundance of mm-sized spherules produced by an impact of a given size, as well as how those spherules are distributed within the ejecta of their source crater.

Despite efforts to detect impact glasses remotely, their abundance and distribution within the ejecta and abundance relative to the crater's size remain unknown for the Moon (Cannon & Mustard, 2015; Schultz & Mustard, 2004; Tompkins & Pieters, 2010). This motivates us to look to the terrestrial impact record for possible constraints on the abundance and distribution of impact glasses in ejecta. The closest terrestrial analogues to the lunar impact spherules used in our observational data shown in Figure 1 are the terrestrial microtektites (Donnelly & Chao, 1973). Microtektites are glassy millimeter-sized or smaller impactites that are morphologically similar to lunar impact glass spherules.

We use observational constraints on the abundance and distribution of terrestrial microtektites relative to their source craters to provide constraints on our glass spherule production model. To do so, we need to understand the relationship between the spatial distribution of spherules relative to their source crater. Because CTEM generates large numbers of craters in a single simulation, it uses a very simplified impact excavation scheme based on the Maxwell Z-model, which connects parcels of ejecta back to the excavation flow within the transient crater (Maxwell, 1977; Maxwell & Seifert, 1974). A 2-D schematic of the simplified model is shown in Figure 2, though in CTEM the calculations are done in 3-D.

For this work we conceptualize spherules (or microtektites) as originating in the melt zone of the transient crater. We only produce spherules in our model arising from resolved primary craters, not secondary craters or subpixel craters. Secondary craters are less energetic and produce little melt (Bjorkman & Holsapple, 1987). While Horz and Cintala (1997) proposed micrometeorites as a source of spherules, we consider this unlikely based on the fact that micrometeorites form agglutinates, which are a distinct kind of melt product from the spherules modeled in our study.

Figure 2a shows the relevant processes in our spherule production model. Inside the transient crater we have include a vapor zone and a melt zone, whose volumes are constrained by Cintala and Grieve (1998) and Abramov et al. (2012). The pixels that make up an ejecta block can be traced back to volumes that are bounded by the streamlines within the transient crater. We further restrict spherule production to occur only in the melt zone for those streamtubes that emerge inward what we call the spherule production onset distance. Because the streamtubes that emerge closest to the impact point have the highest ejection velocity, fresh glass spherules are only distributed in the ejecta outward of a specific range. The onset distance for glass spherule distribution in the ejecta for lunar craters is calculated assuming ballistic flight in lunar gravity from the ejecta launch position given by

$$l(r, R_{tc}) = r + \frac{2v_e^2(r, R_{tc}) \sin \theta_e \cos \theta_e}{g} \tag{1}$$

where $l(r, R_{tc})$ is the ballistic range from impact center as function of launching position (r) and transient crater radius (R_{tc}), $v_e(r, R_{tc})$ is the launching velocity as function of launching position and transient crater size, and

a) Schematic of the glass spherule production model

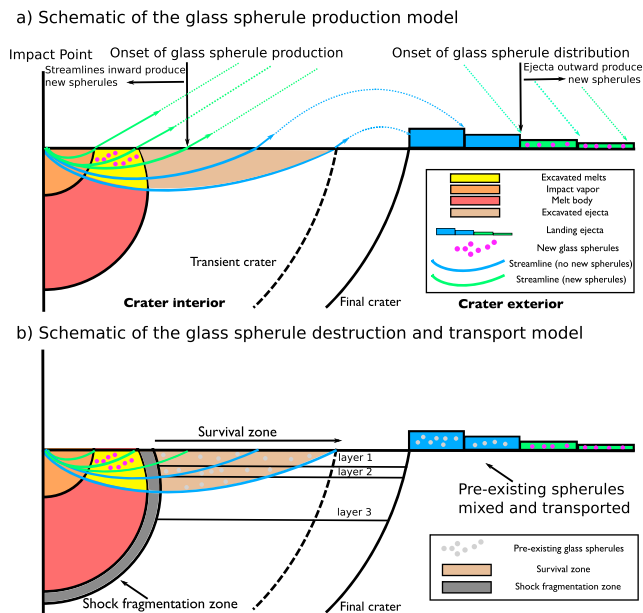b) Schematic of the glass spherule destruction and transport model

Figure 2. An illustration of spherule production, transport, and destruction in Cratered Terrain Evolution Model. (a) Spherules are produced within the melt zone for those streamlines that emerge inward of the onset distance for spherule production. (b) Preexisting spherules within regolith layers are destroyed in the melt and shock fragmentation zone. Old spherules entrained within streamlines that intersect the survival zone are mixed with fresh spherules produced as in (a).

θ_e is launching angle, in which 45° is assumed. Using the Pi theorem of dimensional analysis, the launching velocity of an ejecta can be associated with its source transient crater size (Housen et al., 1983).

Figure 3 shows the maximum sizes of melt products that have been linked to terrestrial craters (see supporting information for details). Using the ballistic range equation, equation (1), we can estimate the provenance of microtektites within the transient crater using the deposition distance of each microtektite strewn field. The results of this calculation for all of the impact-generated melt products with associated craters is plotted as the lower x axis of Figure 3. We can then estimate the equivalent deposition distance of products for the Moon, which shown as the upper x axis of Figure 3.
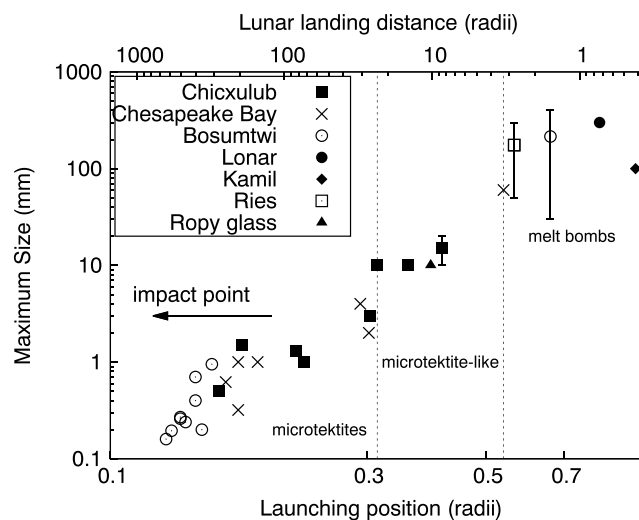
Figure 3. Our modeled impact glass spherule production model based on terrestrial impact crater glass/melt size data. The lower x axis represents the estimated launching position scaled by the calculated transient crater radius. The y axis is the reported maximum size of the impact melt product in millimeters. The upper x axis is the equivalent landing distance under lunar gravity. A full derivation and reference for this data set is included in the supporting information (Text S3).

From Figure 3, there is a relationship between the deposition distance (or equivalently, the launching position) and the size of the melt product. At least three terrestrial impact craters (Lake Bosumtwi, Chesapeake Bay, and Chicxulub Crater) are associated with their microtektite strewn fields (Alvarez et al., 1980; Bohor et al., 1984; Donnelly & Chao, 1973; Glass, 1968; Glass et al., 1973; Smit & Hertogen, 1980). Terrestrial microtektites appear to be more efficiently produced in ejecta deposited farther away from crater centers than nearby crater deposits. For example, several terrestrial microtektite strewn fields are known from deposits obtained from deep drilling in the Pacific Ocean (Glass & Simonson, 2012). From this, we can estimate the onset distance for production of microtektites as 0.3 radii, which becomes an onset distance for spherule deposition of >20 crater radii distance for the Moon (see Figure 2a).

To obtain our onset distances for glass spherule production and distribution, we made many simplifying assumptions. To account for uncertainties we consider in our modeling four different values for our glass distribution onset distances of 0, 5, 10, and 20 crater radii from the rim of the crater. The onset distance of 0 is equivalent to assuming that all ejected melts that were produced during cratering are in the form of mm diameter glass spherules, which is highly unlikely, but we included it to test the limits of our model. Although further investigation is needed to understand the origin of lunar impact glass spherules, our analysis suggests that they are deposited in distal ejecta, and their abundance and scales linearly with crater size. Thus, we applied this simple spherule production model to all sizes of craters in CTEM.

2.2. Modeling the Distribution of Spherule Ages in Lunar Soil Samples

We next simulated a 1-km by 1-km lunar surface with 10-m by 10-m pixels that is subject to 3 Ga of impact bombardment. The area of 1 km by 1 km for our initial simulated surface is roughly on the order of Apollo mission traverse scale; the astronaut traverse scales range from 100 m for Apollo 11 mission to tens of kilometers for Apollo 17 mission. We used a constant bombardment rate with a crater size-frequency distribution as defined by the Neukum Production Function (Neukum et al., 2001).

CTEM generated a few tens of thousands of primary craters in total for each run, ranging from 10 to 500 m in diameter. To track all ejecta that is produced by each crater, CTEM creates a distinct layer for each ejecta blanket at a corresponding deposition distance. This ejecta layer originates in a crater cavity and contains a mixture of transported old spherules as well as fresh spherules (see Figure 2b).

Craters smaller than the 10 m were modeled using subcrater mixing of our layer system. We also model spherules produced by large craters that form outside of the simulated domain, which we call *super-domain* craters, which can be as large as 100-km diameter. During the excavation of each crater on the simulation domain, preexisting spherules in layers at the impact site may be destroyed by melting or shock destruction. Shock destruction of preexisting glass spherules occurs as impact shock pressure exceeds the elastic limit for a glass sphere. We found that other spherule destruction mechanisms, such as spherule breakage caused by high velocity landing, are negligible (see Text S4).

To account for the natural variation from multiple sampling sites from which our observed data set was derived (Figure 1), we performed 50 independent lunar surface simulations. In each individual simulation, we treat each 10-m by 10-m pixel as a model landing site. This yields 500,000 model landing sites from which we derive our model age distribution statistics. Over the course of 3-Ga-long impact bombardment, each model landing site will contain hundreds of ejecta layers in a stack, with each layer containing a unique population of simulated spherules. We mimicked how lunar astronauts scooped up soils by mixing simulated layers at a given pixel down to a specified depth.

We considered this numerical sampling/mixing depth as an additional model parameter, though sampling depths from each of five glass spherule collection in our observed data set were typically <10-cm depth of lunar surface, with the exception of the sample 12023 which was collected from 20 to 23 cm. We tested 10 cm, 1 m, and 3 m for model sampling/mixing depths. The total abundance of glass spherules of a particular age is the weighted average of spherule abundance from all mixed regolith layers down to the sampling/mixing depth.

Our observed data set uses a Gaussian distribution to characterize the relative probability of each individual glass spherule having a particular age, t,

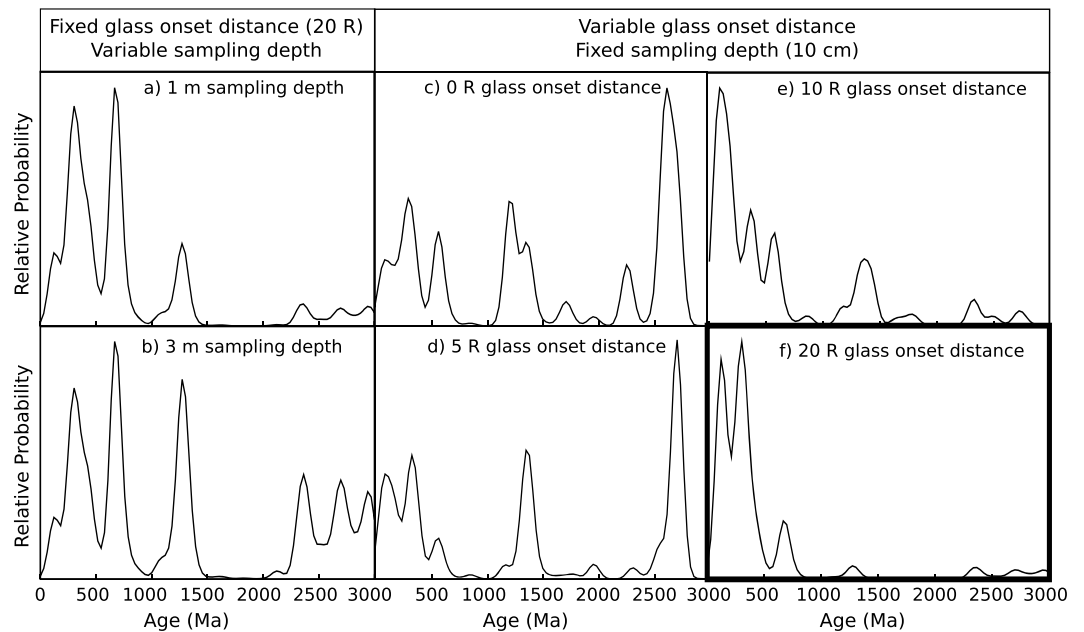$$t = \frac{A}{\sqrt{2\pi}\sigma} \exp\left[-(x-t)^2/2\sigma^2\right],$$

Figure 4. The relative probability plots calculated from all of our 50 simulated surfaces with our two free parameters varied: sampling depth (a and b) and glass distribution onset distance, where R is the crater radius (c–f). The x axis is age (Ma), with the present day at the left. The relative probability of all model samples is calculated in a similar fashion as the observed data set given in Figure 1, but with the constant model resolution σ of 50 Ma.Panel f (highlighted in black, bold line) shows our result with a sampling/mixing depth most similar to the Apollo sampling depth, and with a glass onset distance closest to that from obtained from the terrestrial microtektite constraint. It shows a prominent bias in <500-Ma ages qualitatively similar to our observational data shown in Figure 1.

where A is the amplitude of relative probability of a glass spherule, which is the likelihood of impact events that formed it around the time t, and σ is the analytical error of measured ages of observed impact spherules (<1 Ma to 2 Ga). The median value of age analytical errors from our observed data set is 46 Ma. The amplitude of each glass spherule sample is scaled by the total number of glass spherules. To obtain a relative probability from our model samples, all modeled spherules produced within a 50-Ma interval of time are tagged with the same age.

3. Results

We varied two parameters in our model: the glass onset distance and the sampling/mixing depth. First, we sampled our model spherules to a depth of 10 cm to test how changing the glass onset distance affects the modeled spherule age distribution (see Figures 4c–4f). Next, we fixed the onset distribution distance to 20 radii to test how different model sampling depths affects the modeled spherule age distribution. (see Figures 4a and 4b).

The glass onset distance parameter affects our model spherule age distribution in our model samples for our simulated sampling/mixing depth of 10 cm. If we parameterize the model to distribute glass spherules either at all distances where the ejecta is deposited or beyond the continuous ejecta blanket (2–3 radii), the relative probability of older and younger model spherules is similar (see Figures 4c and 4d).

However, when glass spherules are only generated at >10 radii, the relative probabilities of cratering events as old as 2–3 Ga are reduced (see Figures 4e and 4f). This contrast of relative probabilities between the last 500 Ma and older ages becomes more defined as the onset distance of spherule distribution is increased to 20 radii, leading to a much stronger young age bias. Nevertheless, for the onset distance of >10 radii, and assuming a 10-cm sampling/mixing depth, we reproduce the observed excess in impact glasses with ages <500 Ma.

In addition to the shallow sampling depth of 10 cm, we also modeled sampling/mixing depths up to 3 m, which represents the deepest lunar drilling core sample. For our 3-m sampling/mixing depth case, we found little evidence for a young age bias in the relative probability of the spherule ages. Figure 4a illustrates another age distribution of model samples collected from the depth of 1 m. The relative probability appears to have a young age bias, though not as strong as the 10-cm sampling/mixing depth case. We found that a young age bias in the case of other glass onset distance (e.g., >5 radii) does not correlate well with sampling/mixing depths.

Several older cratering events can still be seen from our shallowly-collected samples, yet the fraction of their population within the depth of 10 cm is much smaller than for the younger cratering events. We found that those spherules typically come from tens of kilometer sized craters that formed very far from the simulated domain. With increasing sampling depth, the magnitudes of relative probabilities for cratering events older >1 Ga become more visible. The age distribution derived from our simulation of deeper sampling (Figure 4b) shows a more uniform distribution of ages, reflecting a less biased record. We also note that the young age bias becomes more severe when the assumed shock damage zone in the model is extended, though sampling depth appears to be the main driver controlling the magnitude of the young age bias.

4. Discussion and Conclusion

Despite uncertainties of our spherule onset distance model, we can quantitatively reproduce the <500-Ma excess in the age distribution of impact glasses seen in Figure 1 under the assumption of a constant impact flux and a shallow sampling depth of 10 cm (Figure 4f). Our results suggest that a young age bias in lunar glass spherule populations strongly correlates with the sampling depth. If the use of terrestrial microtektite data to infer the lunar impact glass spherule distribution onset distance of 20 crater radii is reasonable, then there is a very strong depth-dependent young age bias in the age distribution of spherules, as seen in Figures 4a, 4b, and 4f.

The source of the depth-dependent young age bias is likely related to the process of impact gardening. Ejecta that includes glass spherules deposits on top of older terrain, and subsequent impact events alter the topmost layer of the local surface. This topmost millimeter- and centimeter-thick layer is characterized as being well mixed (Costello et al., 2018; Gault et al., 1974; Hörz & Cintala, 1997; Oberbeck, 1975; Speyerer et al., 2016). This reworking process incorporates a fraction of old deposits into younger deposits.

As older impact events can be readily seen in our model samples from deeper sampling depths, we suggest a shielding effect for older distal ejecta products (>500 Ma) that preserves them against reworking. If the fraction of older glass spherules is minor, it is likely to be diluted by younger ejecta deposits. Over time the tendency of impacts to preferentially rework the topmost layer leads to a concentration of younger ejecta and spherules deposited at the uppermost surface. Using impact glass spherule ages within this reworked zone as a window to the lunar impact flux is prone to this natural bias in the sampling process. The competition between near-surface destruction and burial naturally gives rise to a depth-dependent destruction rate for spherules. As a result, the preexisting glass spherules in a deeper part of surface are shielded. Impact glass spherules at $\gtrsim$1-m depth can become shielded from destruction by impact gardening over the last ~3 Ga. The weaker shielding further implies that the residence time of a glass spherule population in shallower depths is shorter than for deeper depths.

We observed that the residence time of model glass spherule populations within the range of sampling depths between 1 cm and 6 m approximately follow a single half-life exponential function. We computed the half-life for glass spherule preservation for the 10-cm sampling depth to be 118^{+8}_{-12} Ma, while the half-lives of spherule populations at deeper sampling depths can increase to ~2 Ga (see supporting information for details of how we computed half-lives). It should be noted that an individual spherule population may experience anomalous episodes of excavation or ejecta shielding such that a single half-life exponential function will not necessarily fit at any specific location.

To conclude, our modeling results are consistent with the excesses of young impact glass spherule ages in the last 500 Ma being a result of a depth-dependent age bias and the shallow sampling depth of the Apollo regolith samples and that the spherule age distributions are consistent with a constant impact flux over the last 3 Ga.

References

Abramov, O., Wong, S. M., & Kring, D. A. (2012). Differential melt scaling for oblique impacts on terrestrial planets. *Icarus*, *218*(2), 906–916. https://doi.org/10.1016/j.icarus.2011.12.022

Alvarez, L. W., Alvarez, W., Asaro, F., & Michel, H. V. (1980). Extraterrestrial cause for the Cretaceous-Tertiary extinction. *Science*, *208*(4448), 1095–1108. https://doi.org/10.1126/science.208.4448.1095

Bjorkman, M. D., & Holsapple, K. A. (1987). Velocity scaling impact melt volume. *International Journal of Impact Engineering*, *5*(1-4), 155–163. https://doi.org/10.1016/0734-743X(87)90035-2

Bohor, B. F., Foord, E. E., Modreski, P. J., & Triplehorn, D. M. (1984). Mineralogic evidence for an impact event at the Cretaceous-Tertiary boundary. *Science*, *224*, 867–870. https://doi.org/10.1111/j.1945-5100.1995.tb01113.x

Cannon, K. M., & Mustard, J. F. (2015). Preserved glass-rich impactites on Mars. *Geology*, *43*(7), 635–638. https://doi.org/10.1130/G36953.1

Cintala, M. J., & Grieve, R. A. (1998). Scaling impact melting and crater dimensions: Implications for the lunar cratering record. *Meteoritics & Planetary Science*, *33*(4), 889–912. https://doi.org/10.1111/j.1945-5100.1998.tb01695.x

Costello, E. S., Ghent, R. R., & Lucey, P. G. (2018). The mixing of lunar regolith: Vital updates to a canonical model. *Icarus*, *314*, 327–344. https://doi.org/10.1016/j.icarus.2018.05.023

Culler, T. S., Becker, T. A., Muller, R. A., & Renne, P. R. (2000). Lunar impact history from ^{40}Ar/^{39}Ar dating of glass spherules. *Science*, *287*(5459), 1785–1788. https://doi.org/10.1126/science.287.5459.1785

Delano, J. W. (1991). Geochemical comparison of impact glasses from lunar meteorites ALHA81005 and MAC88105 and Apollo 16 regolith 64001. *Geochimica et Cosmochimica Acta*, *55*(11), 3019–3029. https://doi.org/10.1016/0016-7037(91)90470-P

Delano, J., Lindsley, D., & Rudowski, R. (1982). Glasses of impact origin from Apollo 11, 12, 15, and 16—Evidence for fractional vaporization and mare/highland mixing. In *Lunar and Planetary Science Conference Proceedings* (Vol. 12, pp. 339–370). New York: Pergamon.

Donnelly, T., & Chao, E. (1973). Microtektites of late Eocene age from the eastern Caribbean Sea. In N. T. Edgar, J. B. Saunders, et al. (Eds.), *Initial Reports of the Deep Sea Drilling Project* (Vol. 7, pp. 607–672). Washington, DC: US Government Printing Office.

Fassett, C. I., & Thomson, B. J. (2014). Crater degradation on the lunar maria: Topographic diffusion and the rate of erosion on the Moon. *Journal of Geophysical Research: Planets*, *119*, 2255–2271. https://doi.org/10.1002/2014JE004698

Gault, D., Hörz, F., Brownlee, D., & Hartung, J. (1974). Mixing of the lunar regolith. In *Lunar and Planetary Science Conference Proceedings* (Vol. 5, pp. 2365–2386). New York: Pergamon.

Glass, B. P. (1968). Glassy objects (microtektites?) from deep-sea sediments near the Ivory Coast. *Science*, *161*(3844), 891–893. https://doi.org/10.1126/science.161.3844.891

Glass, B. P., Baker, R. N., Storzer, D., & Wagner, G. A. (1973). North American microtektites from the Caribbean sea and their fission track age. *Earth and Planetary Science Letters*, *19*(2), 184–192. https://doi.org/10.1016/0012-821X(73)90113-1

Glass, B. P., & Simonson, B. M. (2012). *Distal impact ejecta layers: A record of large impacts in sedimentary deposits*. Berlin, Heidelberg: Springer-Verlag.

Grieve, R. A. F. (1984). The impact cratering rate in recent time. *Journal of Geophysical Research*, *89*, B403–B408. https://doi.org/10.1029/JB089iS02p0B403

Hartmann, W. K., Quantin, C., & Mangold, N. (2007). Possible long-term decline in impact rates: 2. Lunar impact-melt data regarding impact history. *Icarus*, *186*(1), 11–23. https://doi.org/10.1016/j.icarus.2006.09.009

Hörz, F. (2000). Time-variable cratering rates? *Science*, *288*(5474), 2095–2095. https://doi.org/10.1126/science.288.5474.2093n

Horz, F., & Cintala, M. (1997). Impact experiments related to the evolution of planetary regoliths. *Meteoritics and Planetary Science*, *32*, 179–209. https://doi.org/10.1111/j.1945-5100.1997.tb01259.x

Hörz, F., & Cintala, M. (1997). The Barringer Award Address presented 1996 July 25, Berlin, Germany: Impact experiments related to the evolution of planetary regoliths. *Meteoritics & Planetary Science*, *32*(2), 179–209.

Housen, K., Schmidt, R., & Holsapple, K. (1983). Crater ejecta scaling laws: Fundamental forms based on dimensional analysis. *Journal of Geophysical Research*, *88*(B3), 2485–2499. https://doi.org/10.1029/JB088iB03p02485

Huang, Y.-H., Minton, D. A., Hirabayashi, M., Elliott, J. R., Richardson, J. E., Fassett, C. I., & Zellner, N. E. B. (2017). Heterogeneous impact transport on the Moon. *Journal of Geophysical Research: Planets*, *122*, 1158–1180. https://doi.org/10.1002/2016JE005160

Hui, M. S., Norman, M., & Jourdan, F. (2009). Tracking formation and transport of Apollo 16 lunar impact glasses through chemistry and dating. In W. Short & I. Cairns (Eds.), *Proc. 9th Australian Space Sci. Conf.* (pp. 43–54). Sydney: National Space Society of Australia Ltd.

Korotev, R. L., Zeigler, R. A., & Floss, C. (2010). On the origin of impact glass in the Apollo 16 regolith. *Geochimica et Cosmochimica Acta*, *74*(24), 7362–7388. https://doi.org/10.1016/j.gca.2010.09.020

Levine, J., Becker, T. A., Muller, R. A., & Renne, P. R. (2005). ^{40}Ar/^{39}Ar dating of Apollo 12 impact spherules. *Geophysical Research Letters*, *32*, L15,201. https://doi.org/10.1029/2005GL022874

Maxwell, D. E. (1977). Simple Z model for cratering, ejection, and the overturned flap. In J. Roddy, R. O. Pepin, & R. B. Merill (Eds.), *Impact and explosion cratering: Planetary and terrestrial implications* (pp. 1003–1008). New York: Pergamon.

Maxwell, D., & Seifert, K. (1974). Modeling of cratering, close-in displacements, and ejecta (Tech. Rep.). Washington, DC: Defense Nuclear Agency.

Mazrouei, S., Ghent, R., & Bottke, W. (2015). Has the lunar impact flux rate changed in the past billion years? *Lunar and Planetary Science Conference Proceedings* (Vol. 46, 2331 pp.). The Woodlands, TX.

McEwen, A. S., Moore, J. M., & Shoemaker, E. M. (1997). The Phanerozoic impact cratering rate: Evidence from the farside of the Moon. *Journal of Geophysical Research*, *102*, 9231–9242. https://doi.org/10.1029/97JE00114

Melosh, H., & Vickery, A. (1991). Melt droplet formation in energetic impact events. *Nature*, *350*(6318), 494. https://doi.org/10.1038/350494a0

Minton, D. A., Richardson, J. E., & Fassett, C. I. (2015). Re-examining the main asteroid belt as the primary source of ancient lunar craters. *Icarus*, *247*, 172–190. https://doi.org/10.1016/j.icarus.2014.10.018

Neukum, G. (1983). Meteorite bombardment and dating of planetary surfaces. Dissertation on attaining venia legendi (tenure) in the Geophysics Department in the Faculty of Geological Sciences of the Ludwig-Maximilians University, Munich, West Germany (186 pp.). (translated from German).

Neukum, G., Ivanov, B. A., & Hartmann, W. K. (2001). Cratering records in the inner solar system in relation to the lunar reference system. *Space Science Reviews*, *96*, 55–86. https://doi.org/10.1023/A:1011989004263

Norman, M., Adena, K., & Christy, A. (2012). Provenance and Pb isotopic ages of lunar volcanic and impact glasses from the Apollo 17 landing site. *Australian Journal of Earth Sciences*, *59*(2), 291–306. https://doi.org/10.1080/08120099.2011.615471

Oberbeck, V. R. (1975). The role of ballistic erosion and sedimentation in lunar stratigraphy. *Reviews of Geophysics*, *13*(2), 337–362. https://doi.org/10.1029/RG013i002p00337

Quantin, C., Mangold, N., Hartmann, W. K., & Allemand, P. (2007). Possible long-term decline in impact rates: 1. Martian geological data. *Icarus*, *186*(1), 1–10. https://doi.org/10.1016/j.icarus.2006/07.008

Reid, A. M., Duncan, A. R., & Richardson, S. H. (1977). In search of LKFM, *Lunar and Planetary Science Conference Proceedings* (Vol. 8, pp. 2321–2338). New York: Pergamon.

Richardson, J. E. (2009). Cratering saturation and equilibrium: A new model looks at an old problem. *Icarus*, *204*(2), 697–715. https://doi.org/10.1016/j.icarus.2009.07.029

Robbins, S. J. (2014). New crater calibrations for the lunar crater-age chronology. *Earth and Planetary Science Letters*, *403*, 188–198. https://doi.org/10.1016/j.epsl.2014.06.038

Schultz, P. H., & Mustard, J. F. (2004). Impact melts and glasses on Mars. *Journal of Geophysical Research*, *109*, E01,001. https://doi.org/10.1029/2002JE002025

Shoemaker, E. M., Wolfe, R. F., & Shoemaker, C. S. (1990). Asteroid and comet flux in the neighborhood of Earth. *Geological Society of America Special Papers*, *247*, 155–170. https://doi.org/10.1130/SPE247

Smit, J., & Hertogen, J. (1980). An extraterrestrial event at the Cretaceous-Tertiary boundary. *Nature*, *285*(5762), 198–200. https://doi.org/10.1038/285198a0

Speyerer, E. J., Povilaitis, R. Z., Robinson, M. S., Thomas, P. C., & Wagner, R. V. (2016). Quantifying crater production and regolith overturn on the Moon with temporal imaging. *Nature*, *538*(7624), 215. https://doi.org/10.1038/nature19829

Symes, S. J., Sears, D. W., Akridge, D., Huang, S., & BENOIT, P. H. (1998). The crystalline lunar spherules: Their formation and implications for the origin of meteoritic chondrules. *Meteoritics & Planetary Science*, *33*(1), 13–29. https://doi.org/10.1111/j.1945-5100.1998.tb01604.x

Tera, F., Papanastassiou, D., & Wasserburg, G. (1974). Isotopic evidence for a terminal lunar cataclysm. *Earth and Planetary Science Letters*, *22*(1), 1–21. https://doi.org/10.1016/0012-821X(74)90059-4

Tompkins, S., & Pieters, C. M. (2010). Spectral characteristics of lunar impact melts and inferred mineralogy. *Meteoritics & Planetary Science*, *45*(7), 1152–1169. https://doi.org/10.1111/j.1945-5100.2010.01074.x

Vokrouhlický, D., Bottke, W. F., & Nesvorný, D. (2017). Forming the Flora family: Implications for the near-Earth asteroid population and large terrestrial planet impactors. *The Astronomical Journal*, *153*(4), 172. https://doi.org/10.3847/1538-3881/aa64dc

Zeigler, R. A., Korotev, R. L., Jolliff, B. L., Haskin, L. A., & Floss, C. (2006). The geochemistry and provenance of Apollo 16 mafic glasses. *Geochimica et Cosmochimica Acta*, *70*(24), 6050–6067. https://doi.org/10.1016/j.gca.2006.08.040

Zellner, N., & Delano, J. (2015). ^{40}Ar/^{39}Ar ages of lunar impact glasses: Relationships among ar diffusivity, chemical composition, shape, and size. *Geochimica et Cosmochimica Acta*, *161*, 203–218. https://doi.org/10.1016/j.gca.2015.04.013